

# Single Top and Higgs Production in $e^-p$ collisions

**Mukesh Kumar**

National Institute for Theoretical Physics, School of Physics,  
University of the Witwatersrand, Wits 2050, South Africa.

E-mail: mukesh.kumar@cern.ch

**Abstract.** In this talk I am going to present some studies on the prospects of single top production at the LHeC and double Higgs production at the FCC-he. In particular, we are investigating the  $tbW$  couplings via single top quark production with the introduction of possible anomalous Lorentz structure and the sensitivity of Higgs self coupling ( $\lambda$ ) through double Higgs production. The studies are performed with 60 GeV electron colliding with 7 (50) TeV proton for LHeC (FCC-he).

The single top studies have been done at parton level and we find the sensitivity of the anomalous coupling at 95% C.L, considering 10-1% of systematics. The double Higgs production has been studied with speculated detector parameters and the sensitivity of  $\lambda$  estimated via the cross section study around the Standard Model Higgs self coupling strength ( $\lambda_{SM}$ ) considering 5% systematic error in signal and backgrounds. Effects of non-standard CP-even and CP-odd couplings for  $hhh$ ,  $hWW$  and  $hhWW$  vertices have been studied and constrained at 95% C.L.

## 1. Introduction

In the Standard Model (SM) of particle physics the top quark, the heaviest among all matter particles, and the Higgs boson, a particle responsible for giving masses to all matter particles and gauge bosons, have utmost importance. And hence it has been and still is a challenge for colliders to study different characteristics of these two particles. These characteristics include their charge, mass, interactions and coupling strengths with other particles etc.

In this talk I will briefly review some of the important properties of the top quark and the Higgs boson. From theoretical calculations and results present and past colliders, I will present our predictions in future  $e^-p$  collider known as LHeC (FCC-he) at center of mass energy  $\sqrt{s} \approx 1.3$  (3.5) TeV.

Section 2 is devoted to the top quark studies and sections 3 and 4 for the Higgs boson studies in  $e^-p$  collisions.

## 2. The top quark at the LHeC

In this section I briefly talk about the physics potential of the proposed Large Hadron Electron Collider (LHeC) by estimating the accuracy of anomalous  $Wtb$  couplings in the single anti-top quark production through  $e^-p$  collisions [1]. Within the SM, the  $Wtb$  vertex is purely left-handed. However, the most general lowest dimension CP conserving (in effect of which couplings are real), Lagrangian for this vertex is given by

$$\mathcal{L}_{Wtb} = \frac{g}{\sqrt{2}} \left[ W_\mu \bar{t} \gamma^\mu (V_{tb} f_1^L P_L + f_1^R P_R) b - \frac{1}{2m_W} W_{\mu\nu} \bar{t} \sigma^{\mu\nu} (f_2^L P_L + f_2^R P_R) b \right] + \text{h.c.} \quad (1)$$

Here  $f_1^L = 1 + \Delta f_1^L$ ,  $W_{\mu\nu} = \partial_\mu W_\nu - \partial_\nu W_\mu$ ,  $P_{L,R} = \frac{1}{2}(1 \mp \gamma_5)$  are left- and right-handed projection operators,  $\sigma^{\mu\nu} = i(\gamma^\mu \gamma^\nu - \gamma^\nu \gamma^\mu)/2$  and  $g = e/\sin\theta_W$ . In the SM,  $|V_{tb}| f_1^L \approx 1$ . So, along with  $\Delta f_1^L$  all other couplings  $f_2^L, f_1^R, f_2^R$  vanish at tree-level but are non-zero at higher orders. The constraints on these couplings are the following:

- Assuming only one anomalous coupling to be non-zero at a time:  $-0.13 \leq |V_{tb}| f_1^L \leq 0.03$ ,  $-0.0007 \leq f_1^R \leq 0.0025$ ,  $-0.0015 \leq f_2^L \leq 0.0004$ ,  $-0.15 \leq f_2^R \leq 0.57$  from  $B$  decays;
- Single top production at DØ assuming  $|V_{tb}| f_1^L = 1$ :  $|f_1^R| \leq 0.548$ ,  $|f_2^L| \leq 0.224$ ,  $|f_2^R| \leq 0.347$ ;
- Associated  $tW$  production at LHC through  $\gamma p$  collision:  $|f_1^R| \leq 0.55$ ,  $|f_2^L| \leq 0.22$ ,  $|f_2^R| \leq 0.35$ ;
- ATLAS: asymmetries associated through angular distribution  $\text{Re}(f_1^R) \in [-0.44, 0.48]$ ,  $\text{Re}(f_2^L) \in [-0.24, 0.21]$ ,  $\text{Re}(f_2^R) \in [-0.49, 0.15]$ .

Loop Corrections:

- QCD:  $f_2^R = -6.61 \times 10^{-3}$ ,  $f_2^L = -1.118 \times 10^{-3}$  ( $m_t = 171$  GeV);
- EW:  $f_2^R = -(1.24 \pm 1.23i) \times 10^{-3}$ ,  $f_2^L = -(0.102 \pm 0.014i) \times 10^{-3}$  ( $m_h = 126$  GeV);
- SM:  $f_2^R = -(7.85 \pm 1.23i) \times 10^{-3}$ ,  $f_2^L = -(1.220 \pm 0.014i) \times 10^{-3}$ .

### 2.1. Single anti-top production

We analyze the anti-top production through the hadronic and leptonic decay modes of  $W$ 's as (a)  $e^- p \rightarrow \bar{t} \nu_e, (\bar{t} \rightarrow W^- \bar{b}, W^- \rightarrow jj)$  and (b)  $e^- p \rightarrow \bar{t} \nu_e, (\bar{t} \rightarrow W^- \bar{b}, W^- \rightarrow l \nu_l)$ , respectively. We impose the following selection cuts on events:

- Minimum transverse momenta:  $p_{T_{b,j}} \geq 20$  GeV,  $p_{T_{j,\bar{i}}} \geq 25$  GeV and  $\cancel{E}_T \geq 25$  GeV;
- Pseudorapidities:  $|\eta_{\bar{b},l}| \leq 2.5$  and  $|\eta_j| \leq 2.5$ ;
- Isolation cuts:  $\Delta R_{ij} \geq 0.4$  where  $i, j$  are leptons, light-jets and  $b$ -jets;
- $\Delta\phi_{MET-j} > 0.4$ ,  $\Delta\phi_{MET-l} > 0.4$ ,  $\Delta\phi_{MET-b} > 0.4$  and
- $|m_{j_1 j_2} - m_W| \leq 22$  GeV for hadronic channel.

After estimation of all possible backgrounds in both channels imposing the above selection cuts, we observed high yields of single anti-top quark production with fiducial efficiency of  $\sim 70\%$  and  $\sim 90\%$  in the hadronic and leptonic decay modes of  $W^-$ , respectively.

### 2.2. Estimators and $\chi^2$ analysis

To find the sensitivity of all non-standard couplings, we follow three different approaches based on one dimensional histograms. In the histograms we compare the SM distributions, including all backgrounds, with all non-standard couplings with representative values  $f_1^R = +0.5$ ,  $f_2^L = -0.5$ ,  $f_2^L = +0.5$  and  $f_2^R = +0.5$ . For hadronic modes, we consider six different distributions, namely,  $\Delta\phi_{MET-j_1}$ ,  $\Delta\phi_{MET-b}$ ,  $\Delta\phi_{MET-W}$ ,  $\Delta\phi_{bW}$ ,  $\cos\theta_{bj_1}$  and  $\Delta\eta_{bj_1}$ , while for leptonic modes, there are four different one dimensional histograms used for the analysis  $\Delta\phi_{MET-l}$ ,  $\Delta\phi_{MET-b}$ ,  $\cos\theta_{bl}$  and  $\Delta\eta_{bl}$ .

2.2.1. *Angular Asymmetries from Histograms:* As a preliminary study to get a feel of different chiral and momentum dependence of couplings, following asymmetries are defined:

$$A_{\theta_{ij}} = \frac{N_+^A(\cos \theta_{ij} > 0) - N_-^A(\cos \theta_{ij} < 0)}{N_+^A(\cos \theta_{ij} > 0) + N_-^A(\cos \theta_{ij} < 0)} \quad (2)$$

$$A_{\Delta\eta_{ij}} = \frac{N_+^A(\Delta\eta_{ij} > 0) - N_-^A(\Delta\eta_{ij} < 0)}{N_+^A(\Delta\eta_{ij} > 0) + N_-^A(\Delta\eta_{ij} < 0)} \quad (3)$$

$$A_{\Delta\Phi_{ij}} = \frac{N_+^A(\Delta\phi_{ij} > \frac{\pi}{2}) - N_-^A(\Delta\phi_{ij} < \frac{\pi}{2})}{N_+^A(\Delta\phi_{ij} > \frac{\pi}{2}) + N_-^A(\Delta\phi_{ij} < \frac{\pi}{2})} \quad (4)$$

with  $0 \leq \Delta\phi_{ij} \leq \pi$ . The asymmetry  $A_\alpha$  and its statistical error for  $N_+^A$  and  $N_-^A$  events, where  $N = (N_+^A + N_-^A) = L \cdot \sigma$ , are calculated using the following definition based on binomial distribution:

$$A_\alpha = a \pm \sigma_a, \quad \text{where} \quad (5)$$

$$a = \frac{N_+^A - N_-^A}{N_+^A + N_-^A} \quad \text{and} \quad \sigma_a = \sqrt{\frac{1 - a^2}{L \cdot \sigma}}; \quad (\alpha = \cos \theta_{ij}, \Delta\eta_{ij}, \Delta\Phi_{ij}). \quad (6)$$

Here  $\sigma \equiv \sigma(e^-p \rightarrow \bar{t}\nu, \bar{t} \rightarrow W^- \bar{b}) \times BR(W^- \rightarrow jj/l^- \bar{\nu}) \times \epsilon_b$  is the total cross section in the respective channels after imposing selection cuts and  $\epsilon_b = 0.6$  is the  $b/\bar{b}$  tagging efficiency.

	$A_{\Delta\Phi_{\not{E}_T j_1}}$	$A_{\Delta\Phi_{\not{E}_T \bar{b}}}$	$A_{\Delta\Phi_{\not{E}_T W^-}}$	$A_{\Delta\Phi_{W^- \bar{b}}}$	$A_{\theta_{b j_1}}$	$A_{\Delta\eta_{b j_1}}$
SM + $\sum_i \text{Bkg}_i$	$.532 \pm .003$	$.282 \pm .005$	$.503 \pm .004$	$.799 \pm .003$	$.023 \pm .001$	$-.712 \pm .003$
$f_1^R = +.5$	$.327 \pm .004$	$.231 \pm .004$	$.564 \pm .004$	$.778 \pm .003$	$.0005 \pm .004$	$-.806 \pm .003$
$f_2^L = -.5$	$.528 \pm .004$	$.082 \pm .004$	$.716 \pm .003$	$.748 \pm .003$	$-.196 \pm .004$	$-.868 \pm .002$
$f_2^L = +.5$	$.390 \pm .005$	$.269 \pm .004$	$.585 \pm .004$	$.683 \pm .004$	$.106 \pm .005$	$-.795 \pm .003$
$f_2^R = +.5$	$.330 \pm .004$	$.363 \pm .004$	$.566 \pm .003$	$.656 \pm .003$	$-.197 \pm .004$	$-.823 \pm .002$

Table 1: *Asymmetries and its error associated with the kinematic distributions in hadronic histograms at an integrated luminosity  $L = 100 \text{ fb}^{-1}$ .*

	$A_{\Delta\Phi_{\not{E}_T l_1}}$	$A_{\Delta\Phi_{\not{E}_T \bar{b}}}$	$A_{\theta_{b l_1}}$	$A_{\Delta\eta_{b l_1}}$
SM + $\sum_i \text{Bkg}_i$	$.384 \pm .004$	$.710 \pm .003$	$.551 \pm .006$	$-.765 \pm .007$
$f_1^R = +.5$	$.484 \pm .004$	$.702 \pm .003$	$.332 \pm .006$	$-.821 \pm .003$
$f_2^L = -.5$	$.526 \pm .004$	$.620 \pm .003$	$.410 \pm .006$	$-.831 \pm .002$
$f_2^L = +.5$	$.353 \pm .005$	$.812 \pm .003$	$.392 \pm .007$	$-.850 \pm .003$
$f_2^R = +.5$	$.424 \pm .004$	$.684 \pm .003$	$.507 \pm .005$	$-.809 \pm .003$

Table 2: *Asymmetries and its error associated with the kinematic distributions in leptonic histograms at an integrated luminosity  $L = 100 \text{ fb}^{-1}$ .*

Tables 1 and 2 show how asymmetries are affected due to anomalous couplings of the order  $10^{-1}$ . The asymmetry suggests that the distribution of the cosine of the angle between the tagged  $\bar{b}$  quark and the highest  $p_T$  jet  $j_1$  in the hadronic mode is the most sensitive observable.

2.2.2. *Exclusion contour from bin analysis:* To make the analysis more effective we perform the  $\chi^2$  analysis defined as:

$$\chi^2(f_i, f_j) = \sum_{k=1}^N \left( \frac{\mathcal{N}_k^{\text{exp}} - \mathcal{N}_k^{\text{th}}(f_i, f_j)}{\delta \mathcal{N}_k^{\text{exp}}} \right)^2 \quad (7)$$

where  $\mathcal{N}_k^{\text{th}}(f_i, f_j)$  and  $\mathcal{N}_k^{\text{exp}}$  are the total number of events predicted by the theory involving  $f_i, f_j$  and measured in the experiment for the  $k^{\text{th}}$  bin.  $\delta\mathcal{N}_k^{\text{exp}}$  is the combined statistical and systematic error  $\delta_{\text{sys}}$  in measuring the events for the  $k^{\text{th}}$  bin. If all the coefficients  $f_i$ 's are small, then the experimental result in the  $k^{\text{th}}$  bin should be approximated by the SM and background prediction as

$$\mathcal{N}_k^{\text{exp}} \approx \mathcal{N}_k^{\text{SM}} + \sum_i \mathcal{N}_k^{\text{Bkg}_i} = \mathcal{N}_k^{\text{SM} + \sum_i \text{Bkg}_i}. \quad (8)$$

The error  $\delta\mathcal{N}_k^{\text{SM}}$  can be defined as

$$\delta\mathcal{N}_k^{\text{SM} + \sum \text{Bkg}_i} = \sqrt{\mathcal{N}_k^{\text{SM} + \sum_i \text{Bkg}_i} \left(1 + \delta_{\text{sys}}^2 \mathcal{N}_k^{\text{SM} + \sum_i \text{Bkg}_i}\right)}. \quad (9)$$

The  $\chi^2$  analysis due to un-correlated systematic uncertainties is studied for three representative values of  $\delta_{\text{sys}}$  at 1%, 5% and 10 %, respectively. And the sensitivity of  $|V_{tb}| \Delta f_1^L$  at 95% C.L. is found to be of the order of  $\sim 10^{-3} - 10^{-2}$  with the corresponding variation of 1% - 10% in the systematic error (which includes the luminosity error). The order of the sensitivity for other anomalous couplings varies between  $\sim 10^{-2} - 10^{-1}$  at 95 % C.L.

*2.2.3. Errors and correlations:* Further, defining the combined  $\chi_{\text{comb.}}^2(f_i, f_j)$  and taking into account of luminosity error  $L \equiv \beta\bar{L}, \beta = 1 \pm \Delta\beta$ :

$$\chi_{\text{comb.}}^2(f_i, f_j) \rightarrow \chi_{\text{comb.}}^2(f_i, f_j, \beta) \equiv \sum_{k=1}^m \sum_{i=0}^n \sum_{j=0}^n (f_i - \bar{f}_i) [V^{-1}]_{ij}^k (f_j - \bar{f}_j) + \left(\frac{\beta_k - 1}{\Delta\beta_k}\right)^2, \quad (10)$$

the sensitivity of  $|V_{tb}| \Delta f_1^L \sim 10^{-2}$  and for other couplings it is  $\sim 10^{-4}$  for  $\Delta\beta \geq 5\%$ .

Our analysis shows that the anomalous  $Wtb$  vertex at the LHeC can be probed to a very high accuracy in comparison to all existing limits.

### 3. The Higgs boson at the LHeC

As mentioned in the introduction, the Higgs boson searches are of utmost importance for all the past and present colliders. However, some properties are always needed to be measured accurately and in this respect future colliders also play very important role. In Ref. [2], the authors studied the  $hb\bar{b}$  coupling at LHeC and they demonstrated that the requirement of forward jet tagging in charged current events strongly enhances the signal-to-background ratio. The charged current process at LHeC is following through  $W$ -vector boson fusion and hence one could measure  $hWW$  coupling strength as well. CP properties of the Higgs boson can be determined considering an effective five-dimensional vertex given as [3],

$$\Gamma_{\mu\nu}(p, q) = \frac{g}{M_W} [\lambda(p \cdot q g_{\mu\nu} - p_\nu q_\mu) + i\lambda' \epsilon_{\mu\nu\rho\sigma} p^\rho q^\sigma], \quad (11)$$

where  $\lambda$  and  $\lambda'$  are the effective coupling strengths for the anomalous CP-conserving and the CP-violating operators, respectively. They have shown that the azimuthal angle between missing energy and non- $b$  jet  $\Delta\phi_{MET-J}$  is a powerful and unambiguous probe of anomalous  $hWW$  couplings, both for CP-conserving and violating type.

#### 4. Double Higgs boson production at the FCC-he

Further plan for high-luminosity LHC provides 50 TeV proton and hence LHeC center of mass energy can be increased upto  $\sim 3.5$  TeV with 60 GeV electron, named to be FCC-he. This energy gives an opportunity to probe Higgs self coupling strength  $g_{hhh}^{(1)}$  through double Higgs boson production. In this work we consider the speculated detector parameters and cut-based analysis to get charged-current signal with respect to all possible charged/neutral-current and photo-production backgrounds [4]. A statistical analysis is also performed to find the sensitivity of  $g_{hhh}^{(1)}$  with other effective couplings described with following effective Lagrangian:

$$\mathcal{L}_{hhh}^{(3)} = \frac{m_h^2}{2v}(1 - g_{hhh}^{(1)})h^3 + \frac{1}{2}g_{hhh}^{(2)}h\partial_\mu h\partial^\mu h, \quad (12)$$

$$\begin{aligned} \mathcal{L}_{hWW}^{(3)} = & -\frac{g}{2m_W}g_{hWW}^{(1)}W^{\mu\nu}W_{\mu\nu}^\dagger h - \frac{g}{m_W}\left[g_{hWW}^{(2)}W^\nu\partial^\mu W_{\mu\nu}^\dagger h + \text{h.c.}\right] \\ & -\frac{g}{2m_W}\tilde{g}_{hWW}W^{\mu\nu}\tilde{W}_{\mu\nu}^\dagger h, \end{aligned} \quad (13)$$

$$\begin{aligned} \mathcal{L}_{hhWW}^{(4)} = & -\frac{g^2}{4m_W^2}g_{hhWW}^{(1)}W^{\mu\nu}W_{\mu\nu}^\dagger h^2 - \frac{g^2}{2m_W^2}\left[g_{hhWW}^{(2)}W^\nu\partial^\mu W_{\mu\nu}^\dagger h^2 + \text{h.c.}\right] \\ & -\frac{g^2}{4m_W^2}\tilde{g}_{hhWW}W^{\mu\nu}\tilde{W}_{\mu\nu}^\dagger h^2. \end{aligned} \quad (14)$$

Here  $g_{hhh}^{(1)}$  is defined so that it appears as a multiplicative constant to  $\lambda_{SM}$  i.e;  $\lambda \rightarrow g_{hhh}^{(1)}\lambda_{SM}$  in the expression of electroweak symmetry breaking potential in SM:

$$V(\Phi) = \mu^2\Phi^\dagger\Phi + \lambda(\Phi^\dagger\Phi)^2 \rightarrow \frac{1}{2}m_h^2h^2 + \lambda vh^3 + \frac{\lambda}{4}h^4, \quad (15)$$

where  $\lambda = \lambda_{SM} = m_h^2/(2v^2) \approx 0.13$ .

##### 4.1. Cross section, Detector setup and cut-based analysis

Fiducial cross sections for signal and backgrounds before cut-based analysis are shown in Table 3. For signal we consider the charged current process  $pe^- \rightarrow \nu_e hhj, h \rightarrow b\bar{b}$ . Photo-production background is very important for signal and other charged/neutral-current backgrounds and those backgrounds estimated through ‘‘Equivalent photon approximation structure function’’ which is calculated with ‘‘Improved Weizsaecker-Williams formula’’ [5].

Process	CC (fb)	NC (fb)	PHOTO (fb)
Signal:	$2.40 \times 10^{-1}$		
$b\bar{b}b\bar{b}j$ :	$8.20 \times 10^{-1}$	$3.60 \times 10^{+3}$	$2.85 \times 10^{+3}$
$b\bar{b}j\bar{j}j$ :	$6.50 \times 10^{+3}$	$2.50 \times 10^{+4}$	$1.94 \times 10^{+6}$
$zzj(z \rightarrow b\bar{b})$ :	$7.40 \times 10^{-1}$	$1.65 \times 10^{-2}$	$1.73 \times 10^{-2}$
$t\bar{t}j(\text{hadronic})$ :	$3.30 \times 10^{-1}$	$1.40 \times 10^{+2}$	$3.27 \times 10^{+2}$
$t\bar{t}j(\text{semi-leptonic})$ :	$1.22 \times 10^{-1}$	$4.90 \times 10^{+1}$	$1.05 \times 10^{+2}$

Table 3: Cross sections (in fb):  $E_e = 60$  GeV,  $E_p = 50$  TeV,  $j = qu\bar{u}d\bar{d}s\bar{s}c\bar{c}$ . Initial cuts:  $|\eta| \leq 10$  for jets, leptons and  $b$ ,  $P_T \geq 10$  GeV,  $\Delta R_{\min} = 0.4$  for all particles.

In the detector setup, the maximum rapidity  $|\eta|$  range is up to 7. For the  $b$ -tagging, the jets with  $|\eta| < 5$  and  $p_T > 15$  GeV is taken. The fake rate for a  $c$ -initiated jet and a light jet to the  $b$ -jet is 10% and 1%, respectively. The weight corresponding to the  $b$ -tagging efficiency or fake rate is assigned to each event. Further, following cut flows are taken for analysis:

- Select 4  $b$  + 1-jet:  $p_T^{jet} > 20$  GeV,  $|\eta| < 7$  for  $non$ - $b$ -jets,  $|\eta| < 5$  for  $b$ -jets. The four  $b$  jets must be well separated within  $\Delta R > 0.7$  in case of the overlapped truth matching in the  $b$ -tagging.
- Rejecting leptons with  $p_T^{e^-} > 10$  GeV (to suppress the neutral-current process)
- $\eta_{forward-jet} > 4.0$ , the forward jet as defined as the  $non$ - $b$ -jet which has the largest  $p_T$  after selecting at least 4  $b$ -jets.
- $MET > 40$  GeV and  $\Delta\Phi_{MET-leadingjet} > 0.4$ ,  $\Delta\Phi_{MET-subleadingjet} > 0.4$ .
- Pair the four  $b$ -jets into two pairs and calculate the invariant masses of each pair. The composition of the pairs which has the smallest variance of mass to  $(m_H - 40)$  GeV is chosen. The first pair is defined as  $90 < M_1 < 125$ , which must have the leading  $b$ -jet. The other pair is defined as  $75 < M_2 < 125$ .
- Choosing the invariant mass of all four  $b$ -jets  $> 280$  GeV.

And the significance is calculated with Poisson distribution  $s = \sqrt{2((S+B)\log(1+S/B) - S)}$ . After performing these cut based analysis the signal events are  $\sim 63$  with respect to total background events  $\sim 35$  and  $s = 8.7$ . A 5% systematic error is introduced into signal and backgrounds.

#### 4.2. Statistical analysis

Following the method given in Ref. [6], exclusion limits for  $g_{hhh}^{(1)}$  are calculated. Fig. 1, shows significant behavior of cross section variation with respect to  $g_{hhh}^{(1)}$  which is expected due to interference between resonant and non-resonant Higgs mediation in the charge-current signal process. The 95% upper limits of all effective couplings appear in the Lagrangian 12, 13 and 14 due to cross section influence is also calculated and shown in Fig. 2. The sensitivity of CP-even and odd  $HWW$  effective couplings  $g_{HWW}^{(1)}$  and  $\tilde{g}_{HWW}$  are same as  $g_{hhh}^{(1)} \sim 10^0$ . However for  $g_{hhh}^{(2)} \sim 10^{-3} - 10^{-4}$  and  $g_{hWW}^{(2)}$ ,  $g_{hhWW}^{(1,2)}$ ,  $\tilde{g}_{hhWW}$  are of the order of  $\sim 10^{-2}$ .

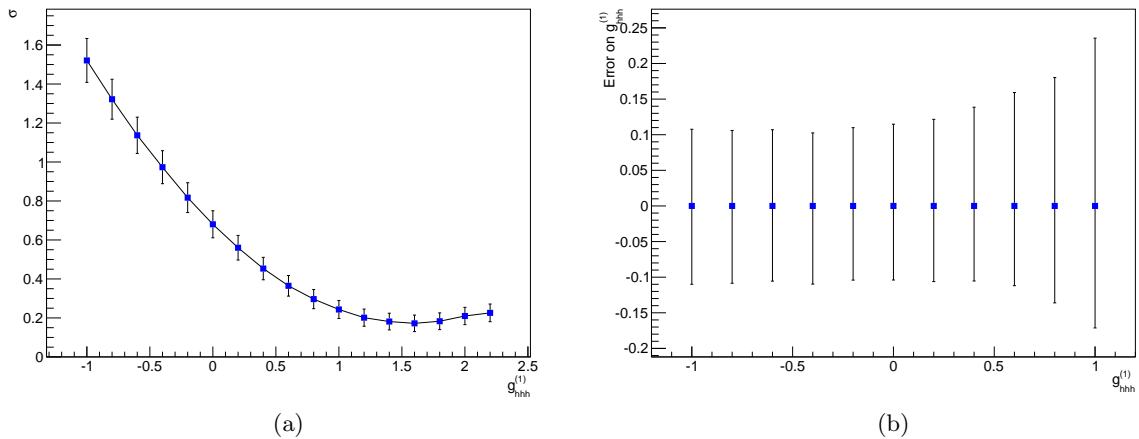


Figure 1: (a) Variation of cross section of the signal process  $\sigma(pe^- \rightarrow \nu_e hhj, h \rightarrow b\bar{b})$  with respect to  $g_{hhh}^{(1)}$  with error bar at each value of  $g_{hhh}^{(1)}$ , (b) local error through linear interpolation at each value of  $g_{hhh}^{(1)}$ .

In conclusion LHeC and FCC-he is a better place to study top and Higgs physics and for the measurement of related couplings to high accuracy.

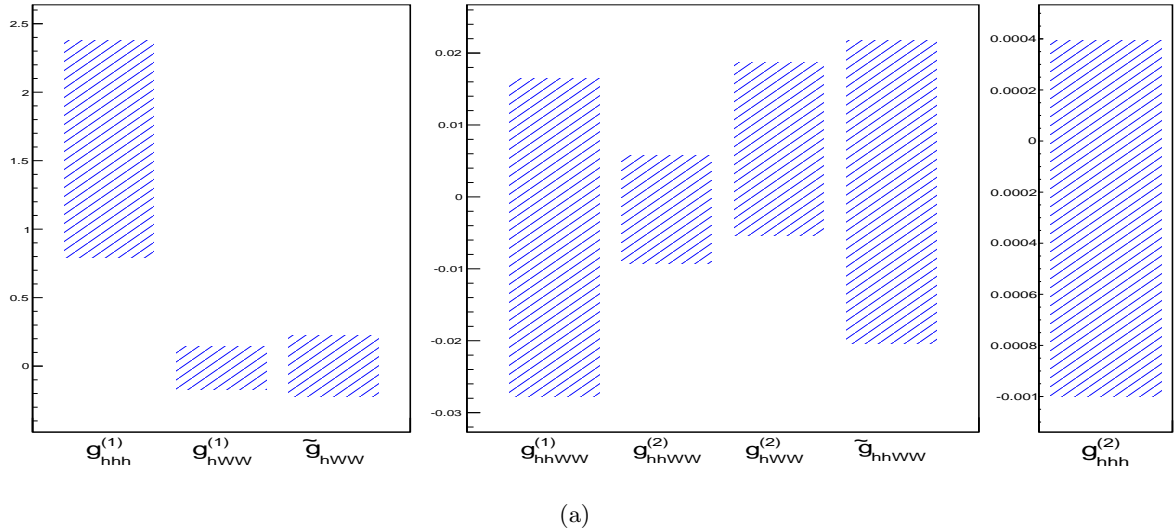


Figure 2: *The limits on the coupling strength, derived at  $0.4 \text{ ab}^{-1}$ . The  $g_{hhh}^{(2)}$  has only the upper limit because the cross section dependence is monotonic in this region.*

### Acknowledgments

MK would like to acknowledge all the collaborators namely Bruce Mellado, Sukanta Dutta, Ashok Goyal, Alan Cornell, Xifeng Ruan and Rashidul Islam and the organisers of the HEPP workshop 2015.

### References

- [1] S. Dutta, A. Goyal, M. Kumar and B. Mellado, arXiv:1307.1688 [hep-ph].
- [2] T. Han and B. Mellado, Phys. Rev. D **82**, 016009 (2010) [arXiv:0909.2460 [hep-ph]].
- [3] S. S. Biswal, R. M. Godbole, B. Mellado and S. Raychaudhuri, Phys. Rev. Lett. **109**, 261801 (2012) [arXiv:1203.6285 [hep-ph]].
- [4] In preparation: M. Kumar, X. Ruan, A. Cornell, R. Islam, M. Klein, U. Klein, B. Mellado
- [5] V. M. Budnev, I. F. Ginzburg, G. V. Meledin and V. G. Serbo, Phys. Rept. **15** (1975) 181.
- [6] G. Cowan, K. Cranmer, E. Gross and O. Vitells, Eur. Phys. J. C **71** (2011) 1554 [Erratum-ibid. C **73** (2013) 2501] [arXiv:1007.1727 [physics.data-an]].